BOREAL ENVIRONMENT RESEARCH 21: 387–404
ISSN 1239-6095 (print) ISSN 1797-2469 (online)

Helsinki 15 February 2016

Stable atmospheric conditions over the Baltic Sea: model evaluation and climatology

Nina Svensson, Hans Bergström, Erik Sahlée and Anna Rutgersson

Department of Earth Sciences, Air, Water and Landscape Sciences, Villavägen 16, SE-752 36 Uppsala, Sweden

Received 22 June 2015, final version received 17 Jan. 2016, accepted 11 Jan. 2016

Svensson N., Bergström H., Sahlée E. & Rutgersson A. 2016: Stable atmospheric conditions over the Baltic Sea: model evaluation and climatology. *Boreal Env. Res.* 21: 387–404.

The WRF (Weather Research and Forecasting model) was evaluated against flight measurements over the Baltic Sea during stable conditions, focusing on vertical profiles of temperature and wind speed. Six different boundary layer parameterization schemes were used. It is shown that there are generally small differences between the boundary layer schemes, and that all schemes have problems in capturing the strength and height of low-level jets. Climatological simulations over the Baltic Sea show that there is a strong seasonality in the stability over the sea with up to 80% stable conditions in spring as compared with 10% in winter. Low-level jets are common, and occur up to 45% of the time in spring. The entire Baltic Sea, not only its coastal areas, is affected by stable stratification.

Introduction

Studies of atmospheric boundary layer processes have for a long time been focused mainly over land areas. Due to the recent growth of the offshore wind industry an increasing amount of measurements are performed offshore, which makes it possible to study the characteristics also of the marine atmospheric boundary layer. Today, the installed wind energy capacity offshore totals nearly 9 GW, or 2% of the total installed wind power, and is expected to keep growing, likely being to be tripled by 2020 (GWEC 2015). This highlights the demand for an accurate description of the wind characteristics over sea surfaces.

This study was focused on the Baltic Sea, where there is a long tradition of research of the marine boundary layer. It is also an area with a potential for increasing wind power development. the Baltic Sea is a semi-enclosed sea, affected to a large degree by the surrounding coasts. The land–sea temperature contrast is often large, being up to 20 °C in spring. The air being advected from land out over the sea affects the marine boundary layer, causing stable conditions in spring, and unstable in autumn and winter (Bergström and Smedman 1999, Dörenkämper *et al*. 2015, Motta *et al*. 2005). Mesoscale phenomena, like sea breeze circulations and low-level jets (LLJ) are created as a result of the temperature contrast between land and sea, and are commonly observed in the Baltic Sea (Källstrand and Smedman 1997). The occurrence of LLJs increases the mean wind speed in an area, but on the other hand causes large wind shear, which affects wind turbines by creating increased blade and rotor loads (Sathe *et al*. 2013). Krogsaeter and Reuder (2015b) showed that the wind shear, even over sea, is higher than

Editor in charge of this article: Veli-Matti Kerminen

the standard wind energy design criterion for a considerable part of the time. Moreover, the roughness change across the coastline induces an internal boundary layer, which in the case of wind speed can be persistent for at least 70 km in stable conditions (Barthelmie *et al*. 2007). In fact, the travel distance for the temperature profile to reach equilibrium with the sea surface can be several hundred kilometers (Smedman *et al*. 1997). In the stable boundary layer, vertical turbulent motions are suppressed, increasing the likelihood of large wind veer with height.

Mesoscale models have been applied to describe the mean conditions in the atmospheric boundary layer with good result, and are a powerful tool for modelling the wind field over a large area, giving insights into the climatology and spatial patterns in meteorological variables that are not possible to obtain from meteorological stations or towers alone. Nevertheless non-neutral atmospheric conditions are challenging to model. In unstable conditions convective eddies cause rapid, non-local transport in the whole boundary layer with high levels of turbulence. Stable conditions are characterized by weak and sometimes intermittent turbulence, gravity waves, low-level jets (Holtslag *et al*. 2013) and anisotropic turbulence (Sukoriansky *et al*. 2005). Boundary layer processes have to be parameterized in these type of models. It is therefore vital to evaluate model results against available measurements under a range of atmospheric conditions and geographical settings. As an example, in a case study by Shin and Hong (2011) it was shown that none of the boundary layer parameterizations could satisfactorily reproduce processes in the stable boundary layer.

In this study the WRF (Weather Research and Forecasting) model (Skamarock *et al*. 2008) is evaluated against flight measurements above the Baltic Sea. Flight measurements give the possibility to obtain measurements over an extended area, and the extent of mesoscale phenomena can be captured both in the horizontal and the vertical, which is a large advantage over point measurements. The aim of this study is to evaluate six commonly used boundary layer schemes in the WRF model, to see if any of them is better at simulating the observed stable conditions over the Baltic Sea. The aim is also to give a view of the climatological characteristics in the area, to show the importance of correct modelling of non-neutral conditions.

The WRF model

WRF is a mesoscale, non-hydrostatic numerical weather prediction model system used widely for research. It can be run with a wide range of physics settings and boundary layer parameterizations. In this study, six commonly used boundary layer schemes will be evaluated; the Mellor-Yamada-Janjic (MYJ) boundary layer scheme (Janjić 1990, 1994), the Mellor-Yamada-Nakanishi-Niino level 2.5 and level 3 (MYNN2 and MYNN3) boundary layer schemes (Nakanishi and Niino 2006, 2009), the Quasi-Normal Scale Elimination (QNSE) boundary layer scheme (Sukoriansky *et al*. 2005), the Yonsei university (YSU) boundary layer scheme (Hong 2010, Hong *et al*. 2006) and the Asymmetric Convection Model 2 (ACM2) boundary layer scheme (Pleim 2007a, 2007b).

Boundary layer schemes are used to compute the sub-grid scale vertical turbulent fluxes of heat, moisture and momentum. Each boundary layer scheme is run with a corresponding surface layer scheme where, if over ocean, the surface fluxes and surface fields are computed using similarity theory. Flux parameterization in weather prediction models is based on gradient diffusion. The YSU and ACM2 schemes have first order closure, meaning that only first order terms are calculated, and the eddy diffusivity is parameterized. The difference between the two schemes is that YSU has a specific treatment of the stable boundary layer, where the diffusivity is determined by a prescribed, parabolic shape function inside the boundary layer. The MYJ, MYNN2 and QNSE schemes have a one-and-a-half order closure, where diffusivity is a function of the time-dependent turbulent kinetic energy (TKE). The rest of the second-order turbulent quantities are diagnosed by gradient diffusion, as is the third order turbulent quantities. MYNN3 is the only tested scheme with a full second order closure. The two MYNN schemes are updated compared with the MYJ scheme, so the turbulent length-scale, closure constants and empirical constants

have new formulations based on a LES database. Another difference in the MYNN schemes is that momentum mixing does not cease above a certain value of the Richardson number, but can take place at strong stability. The QNSE scheme is different from the other TKE schemes because it has scale-dependent diffusivities and viscosities obtained from a spectral closure model. It is designed specifically for stable conditions, and takes into account the anisotropy of stably stratified flow, and can therefore model internal waves in the presence of turbulence.

Boundary layer parameterizations have been shown to have a large impact on model results [*see* for example studies by García-Díez *et al*. (2013), Hahmann *et al*. (2014), Hu *et al*. (2010) and Sterk *et al*. (2013)]. Examples of studies dealing with the differences in boundary layer parameterizations show diverging results. For example, Draxl *et al*. (2012) investigated the differences between the schemes in parameters important for wind energy and found that none of the schemes performed best at all stabilities, but that the MYJ scheme was recommended for stable conditions. Krogsaeter and Reuder (2015b) and Krogsaeter and Reuder (2015a) evaluated WRF data from five boundary layer schemes against a meteorological tower in open water, using one year of data, focusing on wind speed, wind shear and stability. It was found that QNSE and MYJ were the best in simulating wind speed and stability, and that QNSE was the best in reproducing wind shear at stable conditions. Muñoz-Esparza *et al*. (2012) likewise evaluated WRF against this tower, looking separately at unstable, neutral and stable conditions. It was found that for measured stable conditions the model prediction was too neutral. QNSE was again found to be the best scheme in reproducing wind shear at stable conditions. In a case study by Giannakopoulou and Nhili (2014) WRF simulations were evaluated against the same tower for a 2-day stable period, and showed that the MYNN2 scheme was the best scheme in representing these specific conditions. Carvalho *et al*. (2014a) evaluated WRF against measurements at five buoys outside the Portuguese coast using one year of data. In contrast, here it was found that the ACM2 scheme was the best in simulating the wind speed.

The settings and resolution vary between the studies. The horizontal resolutions were 1–5 km, and the vertical resolution was high, in the best case 10 m in the lowest 200 m of the model. There is one exception; in the study by Carvalho *et al*. (2014b), there were only 27 vertical levels with no information of the spacing in the lowest layers, but since they were only simulating surface values this might be adequate enough.

Several authors have also looked at ability of the WRF model to simulate LLJs (e.g., Floors *et al*. 2013, Hu *et al*. 2010, Nunalee and Basu 2013), where it was found that there generally were problems with capturing the height and intensity of LLJs. In their case study of a stable nighttime boundary layer inland Shin and Hong (2011) found that all examined boundary layer schemes underestimated the strength of a LLJ by around 5 m s^{-1}. This was explained to be because the simulated friction velocity and therefore the turbulence levels were too high, which made it difficult to simulate the decoupling from the surface and the connected acceleration of the flow. In contrast, Hu *et al*. (2010) compared the observed and simulated early morning mean wind speed profiles over a 3-month period and found that the ACM2 and MYJ schemes showed a LLJ having higher wind speeds, and with maximum wind speed at lower heights as compared with the observations.

Measurements

Measurements used for model validation consist of air plane measurements conducted over the Baltic Sea surface during two field campaigns. Additional measurements were time series from a meteorological tower at Östergarnsholm, a small island in the Baltic Sea, and were used to give a picture of the weather conditions during the period of the field campaigns.

Östergarnsholm site

Östergarnsholm is a small island situated 4 km off the east coast of Gotland (Fig. 1a). The island is flat and nearly treeless. A meteorological tower is standing on the shore at the southernmost tip

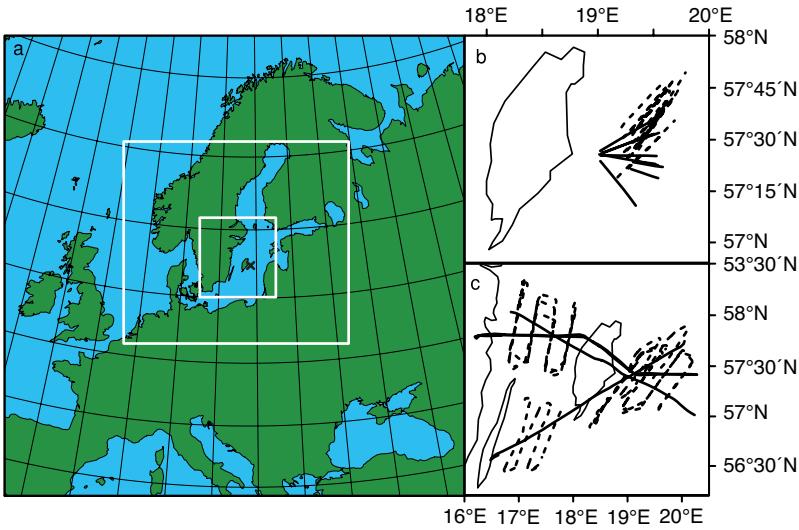

Fig. 1. (**a**) The WRF model domains, where the white boxes represents the inner domains, (**b**) the extent of flight measurements during 1995, and (**c**) 1997. Solid lines show the extent of horizontal flight legs, and dashed lines show locations of slant profiles. The cross in **a** marks the location of the Östergarnsholm tower.

of the island. When the wind is from directions of 80°–220°, there is an open water fetch of more than 150 km. The tower is 30 m high and instrumented with slow response sensors of wind speed, wind direction and temperature at five heights and turbulence sensors at three heights. For a more detailed description of the site, *see* for example Högström *et al*. (2008) or Rutgersson *et al*. (2008). Measurements were also made from a wave-rider buoy situated roughly 5 km SE of Östergarnsholm, which is maintained by the Finnish Institute of Marine Research. Water temperature was measured at 0.5 m below the surface.

Flight measurements

Data from two aircraft measurement campaigns were used in this study. The first campaign (CAMP-95) was part of BALTEX (Baltic sea Experiment), and was conducted during seven days in the period 29 May–15 June 1995, and is described in more detail in Högström *et al*. (1999). It consisted of flight legs at several heights along a line starting outside the east coast of the island Gotland in the Baltic Sea (Fig. 1a) and extending 50 km towards NE, E or SE. The legs were taken at the heights of 30, 60 and 90 m, and above those at 2–5 additional heights, ranging from 200 to 500 m depending on the day. A slant profile was taken before and after each set of horizontal flights (Fig. 1b). The temperature was measured with a temperature probe, wind speed with the radome gust probe technique and the position and speed of the airplane by an inertial navigation system. The wind speed error was estimated to be better than ±0.5 m^{-1} for these flight times and for this aircraft.

The second flight campaign (CAMP-97) was conducted during 1–4 May 1997 by the U.K. Meteorological Office as a part of the EU project STAAARTE (Scientific Training and Access to Aircraft for Atmospheric Research Throughout Europe). The technical details of the airplane and instrumentation is described in Anderson (1997). CAMP-97 also consisted of both horizontal legs and slant profiles. This time measurements were made both east and west of Gotland. Horizontal legs were taken at four heights of around 30, 80, 300/450 and 500/600 m aligned with the mean wind. Sixteen slant profiles were taken along each set of horizontal measurements (Fig. 1c). The air temperature was measured by a Platinum resistance sensor with and accuracy of ±0.3 °C, and sea surface temperature with a pyro electric detector with an accuracy of ±0.5 °C. The wind speed was measured by a pitot-static system with an accuracy of ±0.5 m s^{-1}. In the zoomed-in figures over Gotland horizontal flight legs are shown as full lines and slant profiles as dotted lines.

During both field campaigns stable conditions prevailed due to warm-air advection from

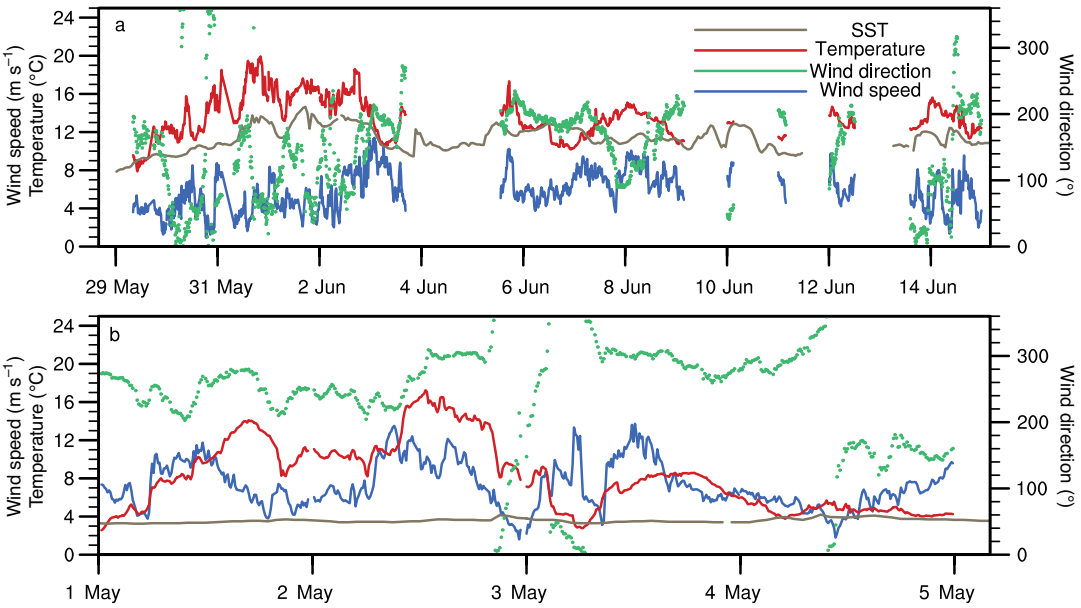

Fig. 2. Time series of wind speed, wind direction and temperature measured at 30 m height from the Östergarnsholm tower and SST from a buoy during (**a**) CAMP-95 and (**b**) CAMP-97.

the surrounding land areas. During CAMP-95 the wind direction according to model simulations was from SE, S or SSW, with winds most often originating from the Polish coast. However, an oscillating behaviour could be seen in the wind direction at the Östergarnsholm site with wind directions varying between southerly and northerly during the course of each day (Fig. 2a). The maximum temperature over land in the upwind area was more than 20 °C and the sea surface temperature ~10 °C at the beginning of the period, creating a land-sea temperature contrast of more than 10 °C. Wind speeds were relatively low with small diurnal variation (Fig. 2a). Högström *et al*. (1999) found that during CAMP-95 the horizontal turbulence structure was quasi-two-dimensional, and to a large degree uncorrelated with the vertical turbulence. The boundary layer was only a few tens of meters deep, and was subject to intermittent shear induced turbulence.

During CAMP-97, the first three days had strong, westerly winds with temperature advection both from the Swedish mainland and from Gotland out over the sea (Fig. 2b). The land–sea temperature contrast was around 9–13 °C. On the last day winds were lower (Fig. 2b), and there was a high pressure ridge across the Baltic Proper, making it possible for LLJs to form. The wind field from this campaign has been modelled before by Källstrand *et al*. (2000) and Törnblom *et al*. (2007), where it was shown that both the roughness and the thermal contrast between land and sea had large impacts on the wind field.

Model simulation set-up

Two sets of simulations with different characteristics were conducted. The first set of simulations (WRF-EVAL) was made to evaluate the model against the flight measurements. This was run with relatively high resolution in order to represent processes in the lower part of the atmosphere with high accuracy. The second set of simulations (WRF-CLIM) covered the years 2000–2013. Because of the long time period, this was run with coarser resolution. However, test simulations with the two resolutions showed only minor differences, which suggests that the results from the WRF-CLIM simulations can be used to show statistics of the general climatological features over the Baltic Sea.

In WRF-EVAL, three model domains were centered over the southern Baltic Sea with the

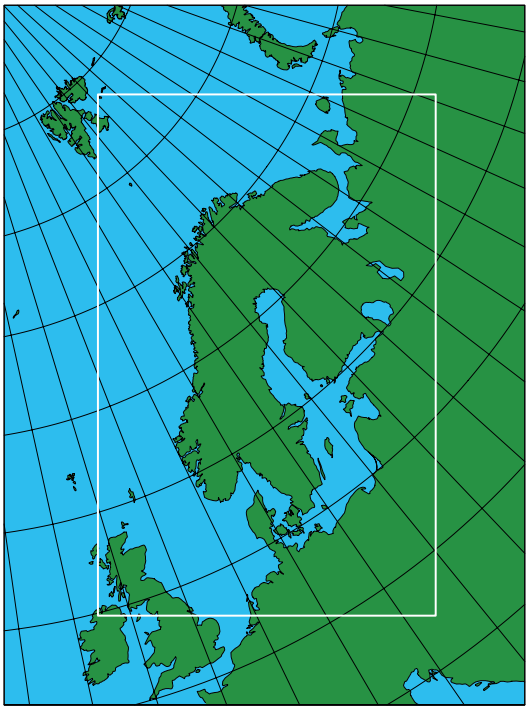

Fig. 3. WRF model domains for the climatological simulation, WRF-CLIM. The white box represents the inner domain.

resolution of 27 × 27 km, 9 × 9 km and 3 × 3 km respectively (Fig. 1a). The results shown here are from the inner domain. The ERA-Interim reanalysis from ECMWF (Dee *et al*. 2011), with 0.75° resolution, was used to force the outer domain every sixth hour. The ERA-Interim data set was chosen because it has been shown to compare well against other data sets (Carvalho *et al*. 2014b, Giannakopoulou and Nhili 2014). There were 48 vertical levels, with 10 levels in the lowest 100 m, in order to get a good representation of boundary layer processes. The simulations were started at 00:00 UTC, and run for up to 18 hours each day.

In order to investigate the differences between WRF boundary layer schemes, six parallel simulations were made, with the six boundary layer schemes and the corresponding surface layer scheme. The rest of the settings were kept constant in all simulations (Table 1).

The WRF-CLIM simulations were run with a coarser resolution in order to be able to cover a longer period. There were two domains, with the innermost centered on the Scandinavian countries (Fig. 3). The ERA-Interim data were used to force the outer domain every sixth hour. The horizontal resolution was 27 and 9 km. The simulations were restarted at 00:00 UTC every day and run for 30 hours, with the first 6 h used as model spin-up time (Table 1).

Results

Five case studies from the airplane measurements are presented here, of which two are examples of warm-air advection with relatively high wind speeds, and three are cases with lower wind speeds that includes a low-level wind speed maximum.

Table 1. Simulation set-up.

Simulation name	Boundary layer scheme	Surface layer scheme	WRF-ARW version	Resolution	Physics options
WRF-EVAL1 WRF-EVAL2 WRF-EVAL3 WRF-EVAL4 WRF-EVAL5 WRF-EVAL6	MYJ MYNN2 MYNN3 QNSE YSU ACM2	Eta similarity MYNN MYNN QNSE MM5 MM5	3.5	Horizontal: 27 × 27 km, 9 × 9 km, 3 × 3 km, vertical: 48 levels	Noah land surface scheme (Tewari *et al.* 2004), Thompson *et al.* (2008) microphysics scheme, RRTM longwave radiation scheme (Mlawer *et al.* 1997), Dudhia (1989) shortwave radiation scheme, Grell (1993) cumulus scheme applied only to outer domain
WRF-CLIM	MYJ	Eta similarity	3.4.1	Horizontal: 27 × 27 km, 9 × 9 km, vertical: 41 levels	Same as above except for the use of Kain-Fritsch cumulus scheme (Kain 2004) on both domains

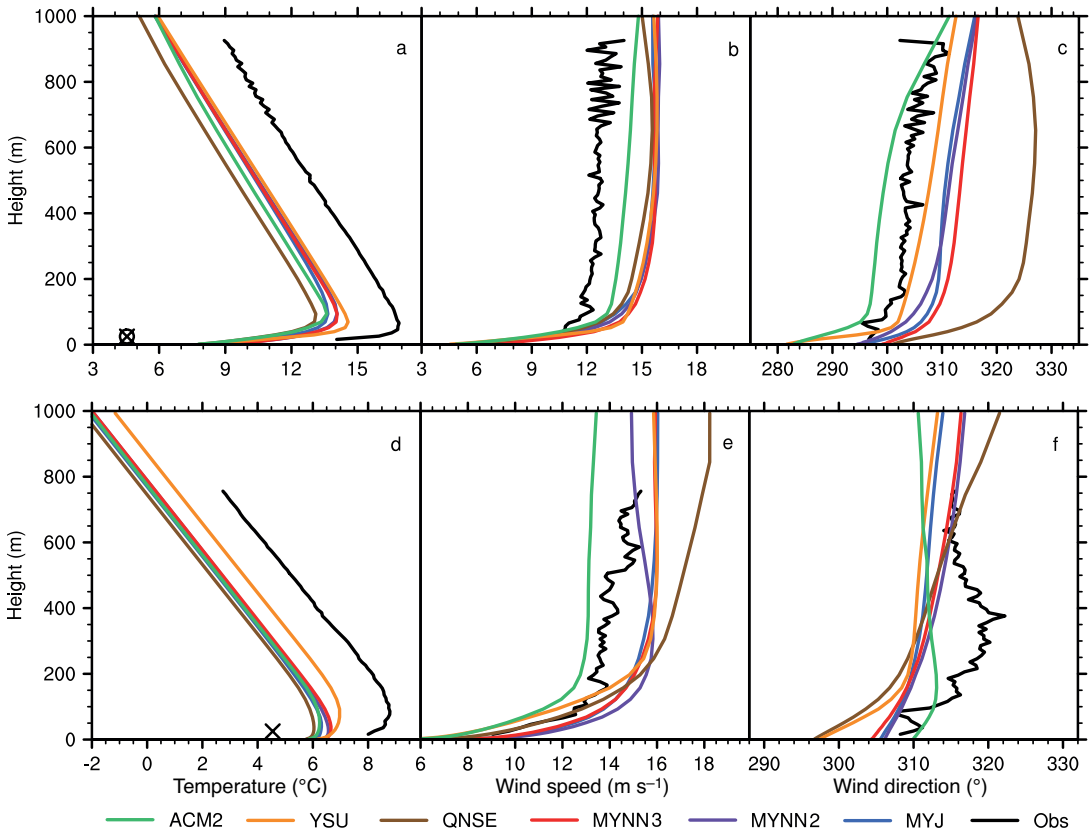

Fig. 4. Mean temperature, wind speed and wind direction profiles from measurements and simulations during (**a–c**) 2 May between 15:13 and 16:15 UTC, and (**d–f**) 3 May between 14:20 and 15:12 UTC. The circle in **a** shows the measured sea surface temperatures; the cross in **a** and **d** shows the modelled sea surface temperature. The measured SST was not available during 3 May.

Warm-air advection cases

The first two cases were taken from 2 May to 3 May from CAMP-97, when warm air was advected out over the sea from the Swedish mainland. The measured profiles of temperature, wind speed and wind direction are combined together with the WRF result (Fig. 4). The measured profiles represent an average over eight slant profiles from the flight measurements from the area between Gotland and the mainland. The profiles were spread out over an area of approximately 70 × 70 km and collected over a period of roughly one hour. The WRF profiles were interpolated to the same location as each of the individual profiles, and then averaged.

During 2 May, there was a very sharp temperature inversion, with its maximum below 100 m height, owing to the short transport distance from the coast and the high land-sea temperature contrast. The wind speed increased with height only in a very shallow layer, up to around 100 m height. During 3 May, a weaker temperature gradient was observed and the wind speed gradient levelled off at higher altitude.

The shape of the temperature profiles was captured quantitatively by the model, although there was a large cold bias in all boundary layer schemes. This bias was largest near the coast, and decreased with distance from the coast in the along-wind direction, indicating an underestimation of the temperature over land, which influenced the temperature profile over sea as well. Comparison with the surface observations from several ground measurement stations (Horn, Malmslätt, Målilla, Ogestad) maintained by SMHI (Swedish Meteorological and Hydrological Institute) showed that the surface tem-

perature was generally underestimated over land in the upwind direction, by up to 3 °C during mid-day (not shown). Similar results were also reported by García-Díez *et al*. (2013), who evaluated the WRF model for one year over continental Europe, showing that there was a general cold bias for all boundary layer schemes during summer, and that especially the maximum temperatures were underestimated. Errors in SST was likely not the cause for the temperature bias. One example is the good agreement between the simulated and measured SST during 2 May (Fig. 4a). Measurements from the buoy outside Östergarnsholm and analyzed charts from SMHI also show that the SST was captured with acceptable accuracy, being 3–4 °C and 4–5 °C respectively during the period of the flight campaign, compared with 4–4.5 °C in the model.

For wind speed and wind direction profiles there were larger differences between the boundary layer schemes than for temperature. Especially the QNSE and ACM2 schemes deviated from the rest of the schemes. The QNSE scheme often shows bulges in the wind speed and direction profiles that are not found in the other schemes.

In addition to the mean profiles, error statistics for the eight profiles in the area is shown for the different boundary layer schemes (Table 2). To capture the error at all heights two types of profile errors were calculated, which corresponds to the mean error (ME) and the mean absolute error (MAE) as an average over thirteen heights. The heights chosen for verification were at 16, 36, 56 m and thereafter increasing in 50 m segments to 400 m and then in 100 m segments up to 700 m. The ME and MAE in wind shear for the different simulations is also given, because it is another measure of the accuracy of the wind speed profile which is important for wind energy. The wind shear is estimated as a maximum difference over 50 m in the lowest 200 m. However, during 2 May, the strongest values of wind shear were often found below 50 m height, and the flight measurements were not always covering these heights. Therefore the error in wind shear could only be calculated for 3 May.

The YSU scheme had the smallest error in temperature, followed by MYNN during both days. QNSE has the largest negative bias and the largest MAE during both days. For the wind speed profile, ACM2 was the best during 2 May, and YSU during 3 May. All simulations showed too low wind shear, i.e. too weak gradients.

The temperature along the flight leg starting over the mainland, and extending eastwards across Gotland is shown for 2 and 3 May 1997 (Fig. 5). The simulations follow the measured temperature in general, with the exception of

Table 2. Error metrics for two warm-air advection cases. The best value in each category is set in boldface.

Boundary layer scheme	Temperature (°C)		Wind speed (m s^{-1})		Maximum wind shear across 50 m, below the height of 200 m (m s^{-1})	
	ME	MAE	ME	MAE	ME	MAE
2 May 1997						
MYJ	–2.3	2.5	1.5	2.1	–	–
MYNN2	**–1.9**	2.2	1.3	2.2	–	–
MYNN3	**–1.9**	2.2	1.3	2.2	–	–
QNSE	–2.6	2.8	1.7	2.1	–	–
YSU	**–1.9**	**1.9**	1.1	2.0	–	–
ACM2	–2.4	2.4	**0.97**	**1.6**	–	–
3 May 1997						
MYJ	–2.4	2.4	0.78	2.3	–0.38	1.1
MYNN2	–2.2	2.2	0.85	2.8	–0.22	**1.0**
MYNN3	–2.2	2.2	0.67	2.6	–0.34	**1.0**
QNSE	–2.6	2.6	0.91	2.3	**–0.13**	**1.0**
YSU	**–1.6**	**1.7**	**0.51**	**2.1**	–0.30	1.2
ACM2	–2.3	2.3	–1.4	2.5	–0.72	1.3

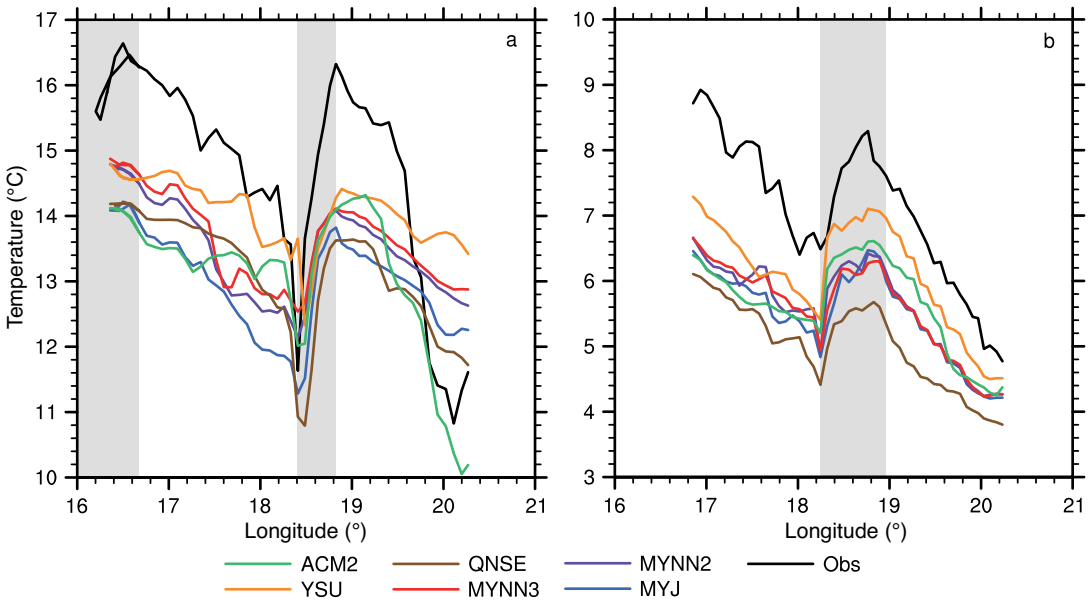

Fig. 5. Temperature at 80 m height from measurements and simulations for (**a**) 2 May, 13:07–14:04 UTC and (**b**) 3 May 12:06–12:54 UTC. The shaded areas mark the location of the mainland and the island of Gotland.

the eastern part of the flight track during 2 May, were all schemes except ACM2 adapt too slowly to the new conditions. In general though, the model can capture the transition from land to sea with the internal boundary layer build-up.

Low-level jet cases

A more or less distinct LLJ was observed in most profiles during CAMP-95. Examples of three clear LLJ cases are shown here (Fig. 6). Temperature and wind speed profiles are shown together with a vertical cross section along the horizontal flight legs from 30 May and 6 June 1995 and 4 May 1997. For CAMP-95, profiles are mean values of the two slant profiles and an average profile calculated from the horizontal flight measurements. For the case from CAMP-97, the profiles are again mean values of all eight slant profiles in the area for that specific set of flights. The dots in the cross-section are shown to give an estimate of the resolution of the horizontal flight measurements, and represent the position of the airplane each minute.

During the first case, a very strong temperature inversion of around 10 °C over the lowest few hundred meters was observed (Fig. 6a). The height of maximum temperature was at a greater altitude as compared with the previous cases (Fig. 4a and d). This was possibly because of the long travel distance across the sea. The upwind distance to the coast was around 200 km, which corresponded to a travel time of 8 h, compared with 0.5–1.5 h in the previous cases. The process of thermal adjustment over the cold sea is described by the theory of Csanady (1974) and was further investigated by Smedman *et al*. (1997) using idealized 2D simulations with a mesoscale model. The theory involves an originally shallow inversion over a cold surface which over time increases in height, and eventually a shallow neutral layer is created near the surface having the same temperature as the sea surface. In the equilibrium condition, there is no heat flux from the air to the water, and the height of the inversion converges to a constant height. The simulations by (Smedman *et al*. 1997) showed that the equilibrium conditions were reached only after several hundred kilometers. According to the Csanady (1974) model, there is a limit in inversion strength above which the neutral layer will never form, which is possibly the case during 30 May. However, in Högström

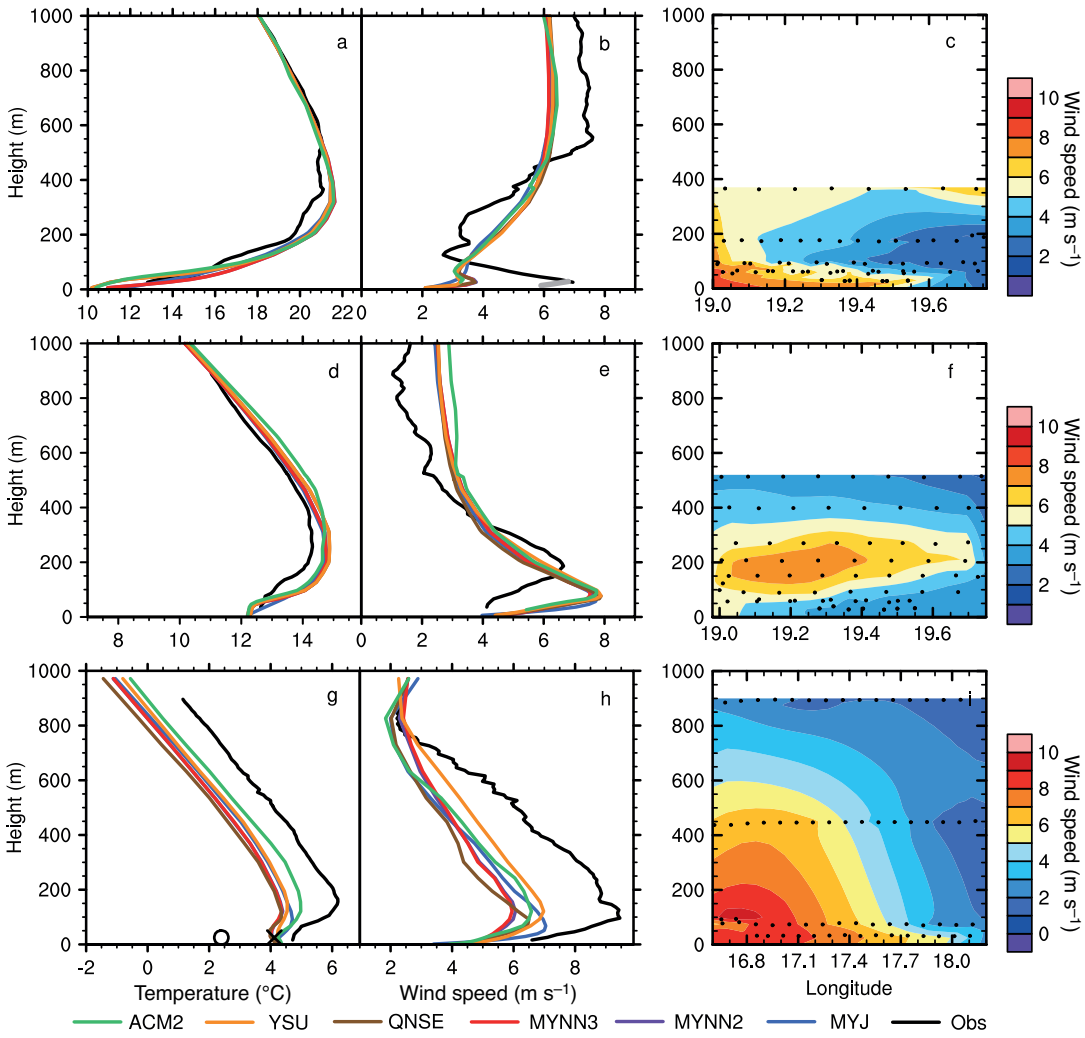

Fig. 6. Mean temperature and wind speed profiles from measurements and simulations, together with a vertical cross-section of the wind speed with longitude interpolated from horizontal flight measurements. The cases are from (**a**–**c**) 30 May 1995, 10:45–12:26 UTC, (**d**–**f**) 6 June 1995, 12:46–14:24 UTC, and (**g**–**i**) 4 May 1997, 15:31–16:44 UTC (profiles) and 11:48–15:23 (horizontal flights). The circle and the cross in **g** show the measured and simulated SSTs, respectively. The dots in the cross-sections show the location of the airplane every minute. The gray profile in **b** shows the wind speed obtained from the Östergarnsholm tower.

et al. (1999) it was argued that the elevated inversion was a result of the increased roughness of Gotland in the upwind direction. Simulations with a mesoscale model showed that if the model was run without any roughness difference between the sea and the island, the temperature inversion was much shallower. At any rate, the modelled temperature agreed well with the observations, and the spread between the boundary layer schemes was very small.

The measured wind profile showed a maximum below 50 m height and a minimum above. The wind direction (not shown) was northwesterly at the height of the LLJ and above there was a strong rightward veer with height of around 120° over a height of few hundred meters. This implies that there was a local mesoscale phenomenon in the area near the island with coast-parallel winds.

The maximum observed wind speed was around 7 m s^{-1} (Fig. 6b and c), which was

also confirmed by measurements at the Östergarnsholm tower. The jet extent from the coast was around 40 km, with the highest wind speeds closest to the coast. From the cross-section it is clear that the jet situation was stationary for some time, because the horizontal measurements, collected during one-and-a-half hour all agree in the shape of the jet. In contrast to measurements, the modelled wind speed profile showed only a very small tendency for a LLJ, with maximum wind speed of 3–4 m s^{-1}. This was true for all boundary layer schemes except for MYJ, where a LLJ could nearly not be seen at all. Similar behaviour of the MYJ scheme was observed by Sterk *et al*. (2013), where it was attributed to its weaker mixing as compared with the YSU and QNSE schemes. The modelled wind direction profile (not shown) was highly veered in a shallow layer below 100 m, and constant above this. This, and the low height of the wind speed maximum suggests that the strength of the momentum mixing in the model was too low for this very stable case, regardless of which boundary layer scheme was used.

The second LLJ occurred on 6 June 1995 (Fig. 6d–f). In this case the temperature inversion was only around 2 °C. Both the measurements and the model showed tendencies for a mixed layer near the surface. However, the height of the mixed layer was significantly lower in the model than in the measurements. One exception was the MYJ scheme, which did not have the mixed layer, but instead showed an inversion. The measured wind speed profile showed a clear wind speed maximum at around 200 m height, extending to 50 km or more from the coast. The wind direction was southerly and only varied around 15 degrees over all heights (not shown). However, the modelled LLJ was 1–1.5 m s^{-1} stronger and the height of the LLJ maximum was around 100 m lower than in the observations. The shape of the modelled temperature and wind speed profiles again suggests that the mixing strength was too low in all schemes.

A third LLJ case was observed on 4 May 1997 (Fig. 6g–i). A mixed layer was seen in temperature profiles both from the measurements and the model below 100 m height, although the temperature gradient was smaller in the model. The near-surface profiles also were better mixed than in the observations, apart from the MYJ scheme. The reason why the MYJ scheme sometimes behave differently as compared with the other schemes can depend on the stability functions used, which are set to zero above a critical Richardson number of 0.25 and therefore inhibiting turbulent mixing at very stable conditions (Cheng *et al*. 2002, Sukoriansky *et al*. 2005). The LLJ had a maximum below 200 m height and covered the whole basin between the mainland and Gotland, a distance of around 80 km. The height of the LLJ was relatively well captured, but the strength was underestimated by 2.5–3.5 m s^{-1}, probably corresponding to the underestimation in stratification.

Error metrics for the three LLJ cases show that different boundary layer schemes scored highest during different days (Table 3). For temperature profiles the MYJ and ACM2 schemes performed best during these days, for wind speed profiles speed it was the YSU and ACM2 schemes. A scheme which is good in simulating LLJs should have low errors in both maximum wind speed, height of maximum wind speed and maximum wind shear, because all these parameters influence the shape of the wind speed profile. There does not seem to be any single scheme that outperforms the others in simulating LLJs. However, the MYJ scheme showed the largest over-prediction in wind shear and largest under-prediction in height during both LLJ days. It is also seen that the boundary layer schemes most often have the same sign of the mean errors, showing that the model error is larger than the difference between the individual schemes.

Results from all flight measurements

In addition to the specific cases presented above, we give a summary of the profile errors in temperature and wind speed for all the available profiles from the two flight campaigns (Table 4). There is not enough data to make the same comparison for wind shear. The errors in wind speed are on average up to 2 m s^{-1} averaged over the profile. Errors in temperature are up to 1.6 °C, but this is mostly due to a cold bias, whereas the shapes of the profiles are often well captured. For temperature profiles YSU has the smallest errors and for wind speed it is the MYJ scheme.

However, differences are small, and no particular scheme outperforms the others. QNSE has the largest errors in temperature, which is in agreement with what was observed in the case studies. Shin and Hong (2011) showed that the QNSE scheme underestimated the daily maximum temperature as compared with three other boundary layer schemes for the convective boundary layer over land, which is in accordance with what is seen here. The differences between the MYNN2 and MYNN3 schemes are small, which is also seen in the case studies. Many authors reported problems with the YSU scheme in stable conditions, showing too neutral profiles. However, this was because of an erroneous implementation of the momentum exchange coefficient, which is now fixed (Hahmann *et al*. 2014, Sterk *et al*. 2013). In their WRF evaluation offshore, Krogsaeter and Reuder (2015b) found that the ACM2 simulated the lowest average wind speed at 100 m height as compared with other boundary layer schemes, which is in accordance with what is seen here. Evaluating the model at several heights increases the confidence in the error estimate, since it is shown from the case studies that the error of, especially wind speed and wind direction, varies with height between the different boundary layer schemes. Due to the relatively short evaluation period it is not possible to draw any conclusions on the better performance of first order or higher order closure schemes, or on which schemes that performs best in stable conditions.

Climatological stability classification in the Baltic Sea

Results from the long-term simulations, WRF-CLIM, are presented here in order to give a

Table 3. Error metrics for temperature and wind speed profiles during 3 days with low level wind maxima. The best value in each category is set in boldface.

Boundary layer scheme	Temperature (°C)		Wind speed (m s^{-1})		Wind speed in LLJ maximum (m s^{-1})		Height of LLJ maximum (m)		Maximum wind shear across 50 m below height of LLJ maximum (m s^{-1})	
	ME	MAE	ME	MAE	ME	MAE	ME	MAE	ME	MAE
30 May 1995										
MYJ	0.41	**0.61**	–0.15	1.6	–	–	–	–	–	–
MYNN2	0.72	0.82	–0.014	1.6	–4.1	4.1	–	–	–	–
MYNN3	0.73	0.82	–0.020	1.6	**–4.0**	**4.0**	–	–	–	–
QNSE	0.62	0.73	0.046	1.6	–4.3	4.3	–	–	–	–
YSU	0.23	0.76	–0.022	1.7	–4.5	4.5	–	–	–	–
ACM2	**0.19**	0.92	**–0.13**	**1.5**	–4.2	4.2	–	–	–	–
6 June 1995										
MYJ	0.34	**0.39**	0.77	1.3	1.0	1.0	–105	105	1.9	1.9
MYNN2	0.32	0.44	0.76	1.3	0.91	0.91	–95	95	0.70	0.70
MYNN3	**0.31**	0.44	0.72	1.3	**0.80**	**0.80**	**–85**	85	0.67	0.67
QNSE	0.32	0.45	**0.60**	1.3	1.2	1.2	–95	95	1.1	1.1
YSU	0.40	0.50	0.83	1.2	1.2	1.2	–90	90	0.89	0.89
ACM2	0.36	0.53	0.65	**1.1**	0.91	0.91	**–85**	85	**0.66**	**0.66**
4 May 1997										
MYJ	–1.3	1.3	–0.97	2.0	–2.8	2.8	–53	53	0.83	1.2
MYNN2	–1.3	1.3	–1.3	2.1	–3.7	3.7	–32	48	–0.93	1.0
MYNN3	–1.3	1.3	–1.3	2.1	–3.8	3.8	10	48	–1.1	1.2
QNSE	–1.6	1.6	–1.2	2.1	–3.2	3.2	–28	48	**0.22**	**0.45**
YSU	–1.1	1.2	**–0.83**	**1.8**	**–2.7**	**2.7**	–6.2	**29**	–0.56	0.90
ACM2	**–0.73**	**0.82**	–1.0	1.9	–2.9	2.9	**–5.0**	48	–0.42	0.75

climatological picture of the temporal and areal extent of stable stratification in the southern Baltic Sea. Hourly values from the years 2000–2013 were divided into stable, near neutral and unstable according to the Richardson gradient number (Ri_G)

$$Ri_G = \frac{g}{\overline{\theta}} \frac{d\theta/dz}{\left(dU/dz\right)^2}, \quad (1)$$

where g is the gravitational constant, θ is the potential temperature, $d\theta/dz$ is the vertical potential temperature gradient and dU/dz is the vertical wind speed gradient between the heights of 6 and 70 m. The Richardson gradient number is divided into stability classes as follows: stable when $Ri_G > 0.05$, near neutral when $-0.05 < Ri_G < 0.05$, and unstable when $Ri_G < -0.05$.

The simulations showed an evident yearly variation, with more than 50% stable conditions in April–July (Fig. 7). During the rest of the year, unstable conditions dominated and there were very few occasions with neutral or near neutral conditions. This agrees with previous stability classifications by Bergström and Smedman (1999) and Guo Larsén (2003) from measurements at the Östergarnsholm site. Motta *et al*. (2005) made a stability classification for the Danish interior seas, and found similar patterns. Krogsaeter and Reuder (2015b) showed, however, that the WRF model tended to overestimate the frequency of occurrence of stable conditions as compared with the observations, with YSU, ACM2 and MYNN2 standing out as the schemes with largest frequency errors of up to 9%. It was also shown from model simulations by Barthelmie *et al*. (2004) that over most parts of the Baltic Proper the yearly mean ratio of stable conditions was 10%–20%. The results from this study yields 20%–40% yearly mean occurrence, which is substantially higher.

To get a picture of the spatial pattern of the atmospheric stratification we present the frequency of occurrence of stable conditions over the southern Baltic Sea during the year (Fig. 8). The reason for not using a standardised seasonal three-month period in the averaging was to better capture the yearly variations with maximum stratification in May. Results presented in Fig. 8 confirm what is shown in Fig. 7, i.e. there was a strong increase in stable conditions during April–May occurring more than 70% of the time in most parts of the Baltic Proper, and not more than 10% in October–December. A striking feature is that the conditions were so spatially homogeneous over the sea surface, showing that the induced stratification from warm-air advection affects the whole basin even far away from the coasts. This was shown to happen for the CAMP-95 case studies, and from the stability classification it is seen that, indeed, it is not uncommon for stable stratification to persist for large over-water distances.

The maximum wind shear over 50 m in the layer from the surface up to 200 m height was also modelled (Fig. 9). A clear yearly variation

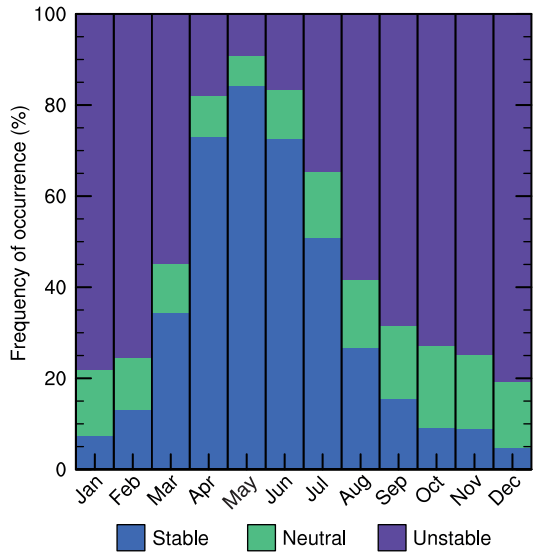

Fig. 7. Average monthly frequency of occurrence of three stability classes at Östergarnsholm.

Table 4. Profile errors for all profiles from the flight campaigns.

Boundary layer scheme	Temperature (°C)		Wind speed (m s^{-1})	
	ME	MAE	ME	MAE
MYJ	–1.3	1.5	**–0.055**	**1.8**
MYNN2	**–1.2**	1.5	–0.19	2.0
MYNN3	**–1.2**	1.5	–0.23	2.0
QNSE	–1.6	1.8	0.10	**1.8**
YSU	**–1.2**	**1.4**	–0.16	**1.8**
ACM2	–1.3	1.5	–0.55	**1.8**

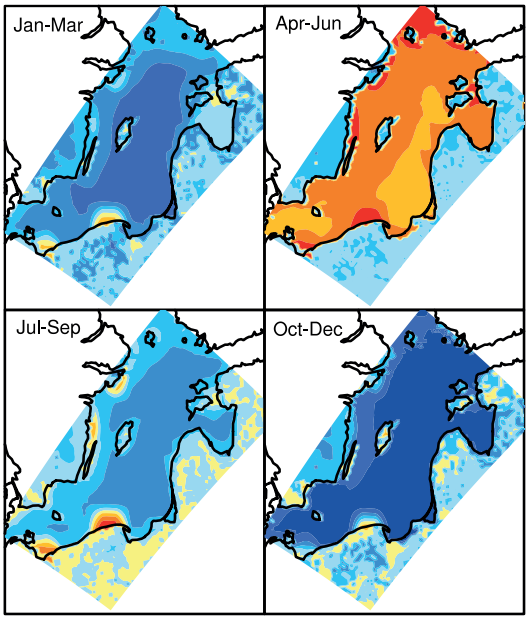

Fig. 8. Frequency of occurrence of stable conditions over the southern Baltic Sea from simulations covering the years 2000–2013.

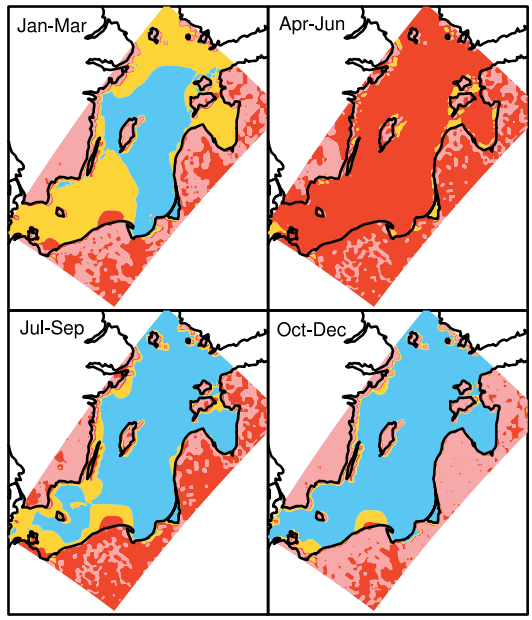

Fig. 9. Maximum shear over 50 m in the lowest 200 m above surface over the southern Baltic Sea from simulations covering the years 2000–2013.

was found with maximum shear in April–June, and much lower shear during the rest of the year. Similarly as for the stratification there were few spatial patterns over the sea surface. However, the maximum wind shear above sea surface was most often lower than the maximum wind shear over land. Dörenkämper *et al*. (2015) calculated the wind shear from observations at the FINO2 tower in the southern Baltic Sea, and showed that in spring there was a 22%–25% increase in wind speed across a height interval of 80 m as compared with 12% in winter. Their results indicate the same patterns as seen here. Dörenkämper *et al*. (2015) also showed that the diurnal peak of the wind shear occurred at 15–22 UTC, at the time when the induced stable stratification resulting from warm-air advection had its peak, showing the close connection between stratification and shear. Similar results as for the wind shear was also found for wind veer (not shown). The average maximum wind veer in April–June was 6°–7° in most parts of the southern Baltic Sea, as compared with 0°–2° in October–December.

Climatology of low-level jets

It is not only the stability itself that affects the wind climate over sea, but also the occurrence of LLJs. Therefore, the frequency of occurrence of LLJs over the Baltic Proper was modelled (Fig. 10). A LLJ in this case was defined as having peak in wind speed which was 2 m s^{-1} higher than the minimum value in a wind speed profile up to 1000 m. Again there was a clear yearly variation, with LLJs being most common in April–June, occurring 45%–50% of the time. The spatial patterns were small for the LLJ occurrence as well, in accordance with the spatial homogeneity of stratification and wind shear, and shows that the Baltic Sea is to a large degree influenced by mesoscale phenomena over its whole extent.

The average height of the LLJ maximum during April–June was 210–250 m, as compared with around 450 m during winter. The average wind speed at the LLJ maximum was 11–12.5 m s^{-1}, as compared with 15–16 m s^{-1} in

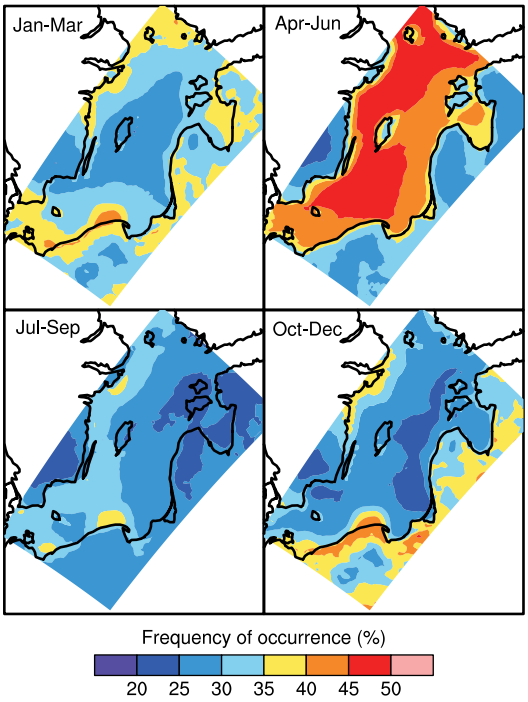

Fig. 10. Frequency of occurrence of LLJs over the southern Baltic Sea from simulations covering the years 2000–2013.

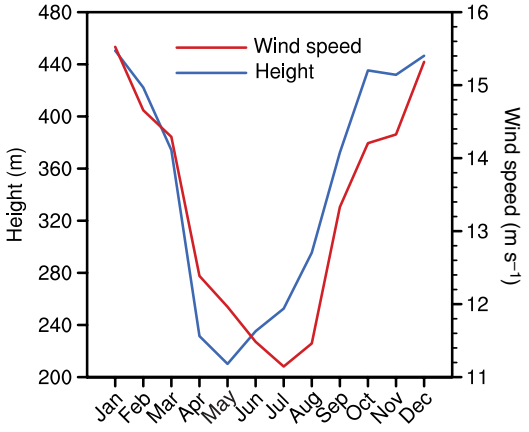

Fig. 11. The average monthly height and wind speed of the LLJ maximum from simulations over the years 2000–2013 at the Östergarnsholm site.

winter (Fig. 11). This shows that the spring LLJs are connected to the stable stratification, with very low boundary layer heights, and as a consequence jet cores confined at low heights. The observed cases shown in earlier section, having jet cores at 50–200 m height, are evidently not uncommon during spring and early summer.

The case studies showed that the height and strength of LLJs was not accurately captured, and this poses an uncertainty on the climatological estimates. The results from the case studies showed that the height of the LLJ was more often under- than overestimated, with differences of up to 100 m as compared with the observations. However, this was during very stable conditions and might not be the case at moderately stable conditions. To obtain accurate information on the height and strength of LLJs more measurements with large vertical extent are needed in coastal or offshore locations. Nevertheless, in the case studies the model produced a well-defined jet at the same time and with the same extent as the measurements. The climatological simulations show a clear trend in connection with the stable conditions and suppressed turbulence, which significantly alters the wind shear at low heights, below 200 m, at heights were modern wind turbines operate.

Conclusions

In this study, the ability of the WRF model to capture the vertical structure in and above the stable boundary layer over sea was investigated. Measurement data consisted of airplane measurements from 9 days with warm air advection out over the Baltic Sea area. It was shown that the shape of temperature, wind speed and wind direction profiles were captured accurately near the coast at relatively high wind speeds. However, the temperature was often underestimated in profiles that had experienced a short travel time from the coast, which was likely due to underestimated temperatures on land. In three case studies of LLJs, it was shown that the strength and height of the LLJ was very hard to capture accurately. In the case of the extremely stable stratification the near ground LLJ was strongly underestimated. A possible reason for this was an underestimation of the mixing in the model, which is also reported by other authors. This was in spite of the high vertical resolution in the lower layers of the model.

The variations in temperature, wind speed and wind direction between the six boundary

layer schemes were generally small. There was a large variability between the days of the field campaigns, and the scheme that was the best one day could be the worst the next day. The MYJ scheme sometimes showed too stable temperature profiles or the absence of a LLJ, which indicates problems with the mixing. This issue was addressed in the design of the MYNN schemes, which shows an improvement over the MYJ scheme. There were rather small differences between the two MYNN schemes in general, showing that there was no large improvement of the higher complexity of the MYNN3 scheme over MYNN2. The QNSE scheme is designed specifically for stable conditions, but did not outperform the other schemes, instead showing relatively similar profiles, and in some cases diverging very much from the measurements. No specific scheme was found to be better at representing stable conditions, and one reason for this was of course the short evaluation period. Nevertheless, this study points out that there is still work to be done in the parameterization of stable conditions.

Results from long-term simulations were used to show the climatological conditions over the Baltic Sea. There were very clear yearly variations in stability, with stable conditions occurring as much as 80% of the time in spring. The whole Baltic Proper was affected by the advection of air from the surrounding coasts. The stable conditions also increased the occurrence of LLJs to a large degree, with as much as 45% occurrence over most of the Baltic Proper. This was also connected to an increase in wind shear and wind veer. However, the WRF model is reported to overpredict stable conditions, but the general picture obtained from the climatology still gives insights into the Baltic Sea offshore environment. The climatology showed that the cases from the flight measurements studied here are not uncommon, and that it is very important to consider the models ability to capture LLJ strength and height, because it can modify the wind field significantly.

As a conclusion, the WRF model was able to simulate much of the strongly stable situations over an offshore area, but future work is needed to accurately capture the height and strength of temperature inversions and LLJs. The wind field over the Baltic Sea Proper is highly influenced by the coast over its whole extent, showing that it is very important to accurately simulate stable conditions.

Acknowledgements: We wish to thank Gunnar Bergström for performing the long-term simulations.

References

Anderson D. 1997. *Meteorological research flight, Mk 2 HERCULES, summary of capability*. MRF Techical Note 21. [Available from Building Y46, DERA, Farnborough, Hampshire, GU14 0LX, UK].

Barthelmie R.J., Badger J., Pryor S.C., Hasager C.B., Christiansen M.B. & Jørgensen B.H. 2007. Offshore coastal wind speed gradients: issues for the design and development of large offshore windfarms. *Wind Engineering* 31: 369–382.

Barthelmie R., Larsen G., Pryor S., Jørgensen H., Bergström H., Schlez W., Rados K., Lange B., Vølund P., Neckelmann S., Mogensen S., Schepers G., Hegberg T., Folkerts L. & Magnusson M. 2004. ENDOW (Efficient Development of Offshore Wind Farms): Modelling wake and boundary layer interactions. *Wind Energy* 7: 225–245.

Bergström H. & Smedman A.-S. 1999. Wind climatology for a well-exposed site in the Baltic Sea. *Wind Engineering* 23: 133–142.

Carvalho D., Rocha A., Gómez-Gesteira M. & Silva Santos C. 2014a. Sensitivity of the WRF model wind simulation and wind energy production estimates to planetary boundary layer parameterizations for onshore and offshore areas in the Iberian Peninsula. *Applied Energy* 135: 234–246.

Carvalho D., Rocha A., Gómez-Gesteira M. & Silva Santos C. 2014b. WRF wind simulation and wind energy production estimates forced by different reanalyses: comparison with observed data for Portugal. *Applied Energy* 117: 116–126.

Cheng Y., Canuto V.M. & Howard A.M. 2002. An improved model for the turbulent PBL. *J. Atmos. Sci.* 59: 1550–1565.

Csanady G.T. 1974. Equilibrium theory of the planetary boundary layer with an inversion lid. *Bound.-Lay. Meteorol.* 6: 63–79.

Dee D.P., Uppala, S.M., Simmons A.J., Berrisford P., Poli P., Kobayashi S., Andrae U., Balmaseda M.A., Balsamo G., Bauer P., Bechtold P., Beljaars A.C.M., van de Berg L., Bidlot J., Bormann N., Delsol C., Dragani R., Fuentes M., Geer A.J., Haimberger L., Healy S.B., Hersbach H., Hólm E.V., Isaksen L., Kållberg P., Köhler M., Matricardi M., McNally A.P., Monge-Sanz B.M., Morcrette J.-J., Park B.-K., Peubey C., de Rosnay P., Tavolato C., Thépaut J.-N. & Vitart F. 2011. The ERA-Interim reanalysis: configuration and performance of the data assimilation system. *Q. J. R. Meteorol. Soc.* 137: 553–597.

Draxl C., Hahmann A.N., Peña A. & Giebel G. 2012. Evaluating winds and vertical wind shear from Weather Research and Forecasting model forecasts using seven planetary boundary layer schemes. *Wind Energy* 17: 39–55.

Dudhia J. 1989. Numerical study of convection observed during the winter monsoon experiment using a mesoscale two-dimensional model. *J. Atmos. Sci.* 46: 3077–3107.

Dörenkämper M., Optis M., Monahan A. & Steinfeld G. 2015. On the offshore advection of boundary-layer structures and the influence on offshore wind conditions. *Bound.-Lay. Meteorol.* 155: 459–482.

Floors R., Vincent C.L., Gryning S., Peña A. & Batchvarova E. 2013. The wind profile in the coastal boundary layer: Wind lidar measurements and numerical modelling. *Bound.-Lay. Meteorol.* 147: 469–491.

García-Díez M., Fernández J., Fita L. & Yagüe C. 2013. Seasonal dependence of WRF model biases and sensitivity to PBL schemes over Europe. *Q. J. R. Meteorol. Soc.* 139: 501–514.

Giannakopoulou E. & Nhili R. 2014. WRF model methodology for offshore wind energy applications. *Adv. Meteorol.* 2014: 1–14.

Grell G.A. 1993. Prognostic evaluation of assumptions used by cumulus parameterizations. *Mon. Weather Rev.* 121: 764–787.

Guo Larsén X. 2003. Air–sea exchange of momentum and sensible heat over the Baltic Sea. *Comprehensive summaries of Uppsala Disserations from the Faculty of Science and Technology* 820: 1–34.

GWEC 2015. *Global wind report — annual market update 2014*. Global Wind Energy Council.

Hahmann A.N., Vincent C.L., Peña A., Lange J. & Hasager C.B. 2014. Wind climate estimation using WRF model output: Method and model sensitivities over the sea. *Int. J. Climatol.* 35: 3422–3439.

Holtslag A.A.M., Svensson G., Baas P., Basu S., Beare B., Beljaars A.C.M., Bosveld F.C., Cuxart J., Lindvall J., Steeneveld G.J., Tjernström M. & van de Wiel B.J.H. 2013. Stable atmospheric boundary layers and diurnal cycles: Challenges for weather and climate models. *Bull. Am. Meteorol. Soc.* 94: 1691–1706.

Hong S.Y. 2010. A new stable boundary-layer mixing scheme and its impact on the simulated East Asian summer monsoon. *Q. J. R. Meteorol. Soc.* 136: 1481–1496.

Hong S.-Y., Noh Y. & Dudhia J. 2006. A new vertical diffusion package with an explicit treatment of entrainment processes. *Mon. Weather Rev.* 134: 2318–2341.

Hu X.M., Nielsen-Gammon J.W. & Zhang F. 2010. Evaluation of three planetary boundary layer schemes in the WRF model. *J. Appl. Meteorol. Clim.* 49: 1831–1844.

Högström U., Sahlée E., Drennan W.M., Kahma K.K., Smedman A.-S., Johansson C., Petterson H., Rutgersson A., Tuomi L., Zhang F. & Johansson M. 2008. Momentum fluxes and wind gradients in the marine boundary layer — a multi-platform study. *Boreal Env. Res.* 13: 475–502.

Högström U., Smedman A.-S. & Bergström H. 1999. A case study of two-dimensional stratified turbulence. *J. Atmos. Sci.* 56: 959–976.

Janjić Z.I. 1990. The step-mountain coordinate: physical package. *Mon. Weather Rev.* 118: 1429–1443.

Janjić Z.I. 1994. The step-mountain eta coordinate model: Further developments of the convection, viscous sublayer, and turbulence closure schemes. *Mon. Weather Rev.* 122: 927–945.

Kain J.S. 2004. The Kain–Fritsch convective parameterization: an update. *J. Appl. Meteorol.* 43: 170–181.

Krogsaeter O. & Reuder J. 2015a. Validation of boundary layer parameterization schemes in the Weather Research and Forecasting (WRF) model under the aspect of offshore wind energy applications — Part II: boundary layer height and atmospheric stability. *Wind Energy* 18: 1291–1302.

Krogsaeter O. & Reuder J. 2015b. Validation of boundary layer parameterization schemes in the weather research and forecasting model under the aspect of offshore wind energy applications — Part I: Average wind speed and wind shear. *Wind Energy* 18: 769–782.

Källstrand B., Bergström H., Højstrup J. & Smedman A.-S. 2000. Mesoscale wind field modifications over the Baltic Sea. *Bound.-Lay. Meteorol.* 95: 161–188.

Källstrand B. & Smedman A.S. 1997. A case study of the near-neutral coastal internal boundary-layer growth: Aircraft measurements compared with different model estimates. *Bound.-Lay. Meteorol.* 85: 1–33.

Mlawer E.J., Taubman S.J., Brown P.D., Iacono M.J. & Clough S.A. 1997. Radiative transfer for inhomogeneous atmospheres: RRTM, a validated correlated-k model for the longwave. *J. Geophys. Res.* 102: 16663–16682.

Motta M., Barthelmie R.J. & Vølund P. 2005. The influence of non-logarithmic wind speed profiles on potential power output at danish offshore sites. *Wind Energy* 8: 219–236.

Muñoz-Esparza D., Cañadillas B., Neumann T. & van Beeck J. 2012. Turbulent fluxes, stability and shear in the offshore environment: mesoscale modelling and field observations at FINO1. *Journal of Renewable and Sustainable Energy* 4, 063136, doi: 10.1063/1.4769201.

Nakanishi M. & Niino H. 2006. An improved Mellor-Yamada Level-3 model: its numerical stability and application to a regional prediction of advection fog. *Bound.-Lay. Meteorol.* 119: 397–407.

Nakanishi M. & Niino H. 2009. Development of an improved turbulence closure model for the atmospheric boundary layer. *J. Meteorol. Soc. Jpn.* 87: 895–912.

Nunalee C.G. & Basu S. 2013. Mesoscale modeling of coastal low-level jets: Implications for offshore wind resource estimation. *Wind Energy* 17: 1199–1216.

Pleim J.E. 2007a. A combined local and nonlocal closure model for the atmospheric boundary layer. Part I: Model description and testing. *J. Appl. Meteorol. Clim.* 46: 1383–1395.

Pleim J.E. 2007b. A combined local and nonlocal closure model for the atmospheric boundary layer. Part II: Application and evaluation in a mesoscale meteorological model. *J. Appl. Meteorol. Clim.* 46: 1396–1409.

Rutgersson A., Norman M., Schneider B., Pettersson H. & Sahlée E. 2008. The annual cycle of carbon dioxide and parameters influencing the air–sea carbon exchange in

the Baltic Proper. *J. Marine Syst*. 74: 381–394.

Sathe A., Mann J., Barlas T., Bierbooms W.A.A.M. & van Bussel G.J.W. 2013. Influence of atmospheric stability on wind turbine loads. *Wind Energy* 16: 1013–1032.

Shin H.H. & Hong S.Y. 2011. Intercomparison of planetary boundary-layer parametrizations in the WRF model for a single day from CASES-99. *Bound.-Lay. Meteorol*. 139: 261–281.

Skamarock W.C., Klemp J.B., Dudhia J., Gill D.O., Barker D.M., Duda M.G., Huang X.-Y. Wang W. & Powers J.G. 2008. *A description of the advanced research WRF version 3*. NCAR Technical Note.

Smedman A.-S., Bergström H. & Grisogono B. 1997. Evolution of stable internal boundary layers over a cold sea. *J. Geophys. Res*. 102: 1091–1099.

Sterk H.A.M., Steeneveld G.J. & Holtslag A.A.M. 2013. The role of snow-surface coupling, radiation, and turbulent mixing in modeling a stable boundary layer over Arctic sea ice. *J. Geophys. Res.-Atmos*. 118: 1199–1217.

Sukoriansky S., Galperin B. & Perov V. 2005. Application of a new spectral theory of stably stratified turbulence to the atmospheric boundary layer over sea ice. *Bound.-Lay. Meteorol*. 117: 231–257.

Tewari M., Chen F., Wang W., Dudhia J., Lemone M.A., Mitchell K.E., Ek M., Gayno G., Wegiel J.W. & Cuenca R. 2004. Implementation and verification of the unified NOAH land surface model in the WRF model. In: *20th Conference on Weather Analysis and Forecasting/16th Conference on Numerical Weather Prediction*, *Seattle, WA*, American Meteorological Society, pp. 11–15.

Thompson G., Field P.R., Rasmussen R.M. & Hall W.D. 2008. Explicit forecasts of winter precipitation using an improved bulk microphysics scheme. Part II: Implementation of a new snow parameterization. *Mon. Weather Rev*. 136: 5095–5115.

Törnblom K., Bergström H. & Johansson C. 2007. Thermally driven mesoscale flows — simulations and measurements. *Boreal Env. Res*. 12: 623–641.